Synextensional Pliocene–Pleistocene eruptive activity in the Camargo volcanic field, Chihuahua, México

José Jorge Aranda-Gómez[†]
Centro de Geociencias, Universidad Nacional Autónoma de México, Campus Juriquilla, P.O. Box 1-742, Querétaro, Querétaro 76001, México

James F. Luhr[‡]
Department of Mineral Sciences, NHB-119, Smithsonian Institution, Washington, D.C. 20560, USA

Todd B. Housh[§]
Department of Geological Sciences, University of Texas at Austin, Austin, Texas 78712, USA

Charles B. Connor[#]
Department of Geology, University of South Florida, Tampa, Florida 33620, USA

Tim Becker[††]
Berkeley Geochronology Center, Berkeley, California 94709, USA

Christopher D. Henry[‡‡]
Nevada Bureau of Mines and Geology, University of Nevada, Reno, Nevada 89557-0088, USA

ABSTRACT

The Camargo volcanic field is the largest mafic alkalic volcanic field in the Mexican Basin and Range province, and the relationship between volcanism and normal faulting is especially strong. The Camargo volcanic field lies in the northern part of the province, midway between the Sierra Madre Occidental and Trans-Pecos Texas. It is formed by Pliocene–Pleistocene (4.7–0.09 Ma) intraplate mafic alkalic volcanic rocks, some of which contain peridotite, pyroxenite, and granulite xenoliths. The volcanic field covers ~3000 km² and has an estimated volume of ~120 km³ erupted from >300 recognized vents. Twenty-six new $^{40}Ar/^{39}Ar$ age determinations for the Camargo volcanic field and its environs show that volcanic activity began in the southwest part of the field and shifted toward the northeast at ~15 mm/yr. The average magmatic eruption rate during growth of the field was ~0.026 km³/k.y.

The Camargo volcanic field lies within an accommodation zone with west-dipping faults and east-tilted blocks to the north and east-dipping faults and west-tilted blocks to the south. These faults are expressed in the volcanic field by a N30°W-trending graben with scarps up to ~100 m high through its central part. Volcanism and faulting were at least in part coeval, and younger volcanic products commonly drape fault scarps that cut earlier lavas. Normal faulting is bracketed between 4.7 and 2.1 Ma and may have also migrated northeastward. Estimated vertical slip rates on four Pliocene faults range from 0.03 mm/yr, a likely long-term rate, to 1.67 mm/yr, interpreted as a short-term rate operative during periods of active faulting. Northwest-striking normal faults that cut alluvial-fan deposits and Pleistocene lavas in the northern Camargo volcanic field and geomorphic evidence for recent uplift to the south of the volcanic field suggest that the region is still extending.

Keywords: Basin and Range province, Chihuahua, Mexico, extension faults, intraplate, Pliocene, slip rates.

INTRODUCTION

Continental rift zones are associated worldwide with alkalic volcanic rocks (Bailey, 1974). Despite this broad association between extensional faulting and volcanic activity, the detailed interplay between these two phenomena can be highly variable and equally highly debated. This dichotomy is most notable for the Basin and Range province. In the eastern Great Basin, Gans et al. (1989) noted a correlation between the peak of felsic ash-flow tuff eruptions and the abrupt onset of large-magnitude extension. According to their model, eruption of mafic magmas followed as slower, broadly distributed extension set in. In contrast, Axen et al. (1993) concluded that the onset of extension preceded volcanism in some areas, was coincident with volcanism in others, and postdated volcanism in still other parts of the eastern Great Basin. Glazner and Bartley (1994) offered an even more contrary position against a close association between extension and alkalic magmatism in their interpretation that mafic alkalic volcanic rocks with peridotite xenoliths from the Mojave Desert erupted during contractional or transpressional deformation.

The Oligocene ''ignimbrite flare-up'' of the Sierra Madre Occidental of Mexico, the largest continuous rhyolite province in the world (Swanson et al., 1978), coincided in time and space with brief pulses of rapid extension. This activity marked the transition from east-northeast compression, related to eastward

[†]E-mail: jjag@servidor.unam.mx.
[‡]E-mail: luhr@volcano.si.edu.
[§]E-mail: housh@mail.utexas.edu.
[#]E-mail: cconnor@chuma1.cas.usf.edu.
[††]E-mail: tbecker@bgc.org.
[‡‡]E-mail: chenry@unr.edu.

GSA Bulletin; March 2003; v. 115; no. 3; p. 298–313; 9 figures; 2 tables; Data Repository item 2003033.

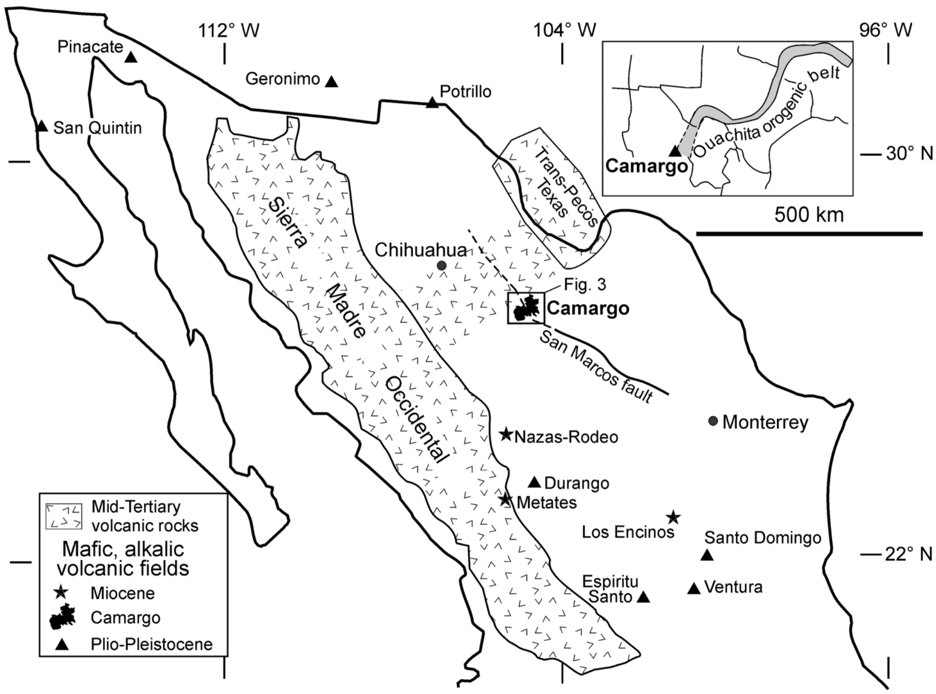

Figure 1. Location of the Camargo volcanic field and its relationship to major tectonic and magmatic features of the region. A belt of Cenozoic volcanic rocks extends between the Sierra Madre Occidental and Trans-Pecos Texas. The trace of the San Marcos fault (solid line) was taken from McKee et al. (1984, 1990), and its inferred extension (dashed line) was taken from Padilla y Sánchez (1986). Inset shows the Ouachita orogenic belt in the south-central United States and its probable continuation in Chihuahua (simplified after Sedlock et al., 1993).

subduction of the Farallon plate, to the east-northeast extension that has since dominated the Mexican Basin and Range province (McDowell and Keizer, 1977; Aguirre-Díaz and McDowell, 1991; Nieto-Samaniego et al., 1999; Luhr et al., 2001). This felsic volcanism and coeval faulting are consistent with the model of Gans et al. (1989), as is the subsequent Miocene–Quaternary mafic alkalic magmatism. Among the major mafic alkalic volcanic fields of the Mexican Basin and Range province, we have investigated three Miocene and four Quaternary examples. In the 24 Ma Rodeo field of Durango State (Fig. 1), hawaiites are interbedded with graben-fill gravel and are cut by the Rodeo fault, demonstrating their synextensional nature (Luhr et al., 2001). South of Rodeo, the ca. 12 Ma Metates hawaiites (Fig. 1) are similarly underlain by gravels and displaced up to 60 m by normal faulting in the Río Chico graben (Aranda-Gómez et al., 1997; Henry and Aranda-Gómez, 2000). Among the Quaternary volcanic fields, only the relatively large and voluminous Durango volcanic field (Fig. 1) shows evidence of synchronous faulting and eruptive activity. Several northwest-striking normal faults cut the field with scarps up to a few tens of meters high, and Quaternary vent alignments parallel some faults (Aranda-Gómez et al., 1997). In the other Quaternary volcanic fields we have investigated, however, no clear relationship is evident on the surface between volcanism and faulting (Ventura and Santo Domingo: Luhr et al., 1989; San Quintín: Luhr et al., 1995b). However, geophysical data suggest that San Quintín is located in a transtensional basin (Almeida-Vega et al., 2000).

In this paper we describe the geology, age, and structure of the Pliocene–Pleistocene Camargo volcanic field of Chihuahua, the most voluminous mafic alkalic volcanic field in the Mexican Basin and Range province. We also seek to answer the question, How did volcanic activity and normal faulting interplay during the evolution of the Camargo volcanic field? Volcanism and extension are distinctly evident in the central part of the volcanic field, where the lava plains and individual vents are cut by numerous faults (Fig. 2). These structures are, in turn, partly covered by younger volcanic rocks. Ages for the syneruptive normal faulting can be bracketed in many localities, and vertical slip rates can be estimated for various faults. Furthermore, regional structures and faulting appear to have determined the location of the Camargo volcanic field, which lies within an antithetic transfer zone (Peacock and Sanderson, 1997) between two basin-and-range structures where the transfer zone coincides with the regional San Marcos fault (Fig. 1).

REGIONAL TECTONIC SETTING

The Camargo volcanic field is located in southeastern Chihuahua State, east of the Sierra Madre Occidental, at the juncture of several Proterozoic to Mesozoic basement structures that influence its location (Figs. 1 and 2). Scattered outcrops and well data in northern Chihuahua demonstrate the presence of Grenvillian basement, presumably part of the North American craton. At two locations in southeastern Chihuahua, Grenvillian basement is overlain by Paleozoic rocks. These may be part of the Ouachita belt, which can be traced on the surface in west Texas and disappears south of the México–United States border (Fig. 1, inset), under a thick cover of younger sedimentary and volcanic rocks. The edge of the ''nonaccreted continental rocks'' proposed by Coney and Campa (1987) and the extrapolated Ouachita thrust front lie a short distance north of the Camargo volcanic field. Thus, the southern edge of autochthonous Proterozoic North America and the late Paleozoic suture between Laurentia and Gondwana are thought to be near the Camargo volcanic field (Cameron and Jones, 1993).

The Camargo volcanic field is located near the San Marcos fault, which is a major structure that can be traced on the surface for ~300 km (Fig. 1) across the state of Coahuila. At the Chihuahua-Coahuila state line, the fault trace appears to end abruptly against the eastern branch of the Bolsón de Mapimí, a major Basin and Range structure (Fig. 2). Padilla y Sánchez (1986) and Grajales-Nishimura et al. (1992) interpreted that the San Marcos fault may be traced another 250 km northwestward through and past the Camargo volcanic field (Fig. 1). The San Marcos fault has a complex history (McKee and Jones, 1979; McKee et al., 1984, 1990), and it appears that since the Jurassic, it has been reactivated during each of the major pulses of deformation in the region.

The topography of the Camargo volcanic field region reflects both Laramide and Basin and Range deformation. Ranges adjacent to the Camargo volcanic field are occupied by folded Jurassic and Cretaceous rocks that are overlain by a variety of faulted and tilted Ter-

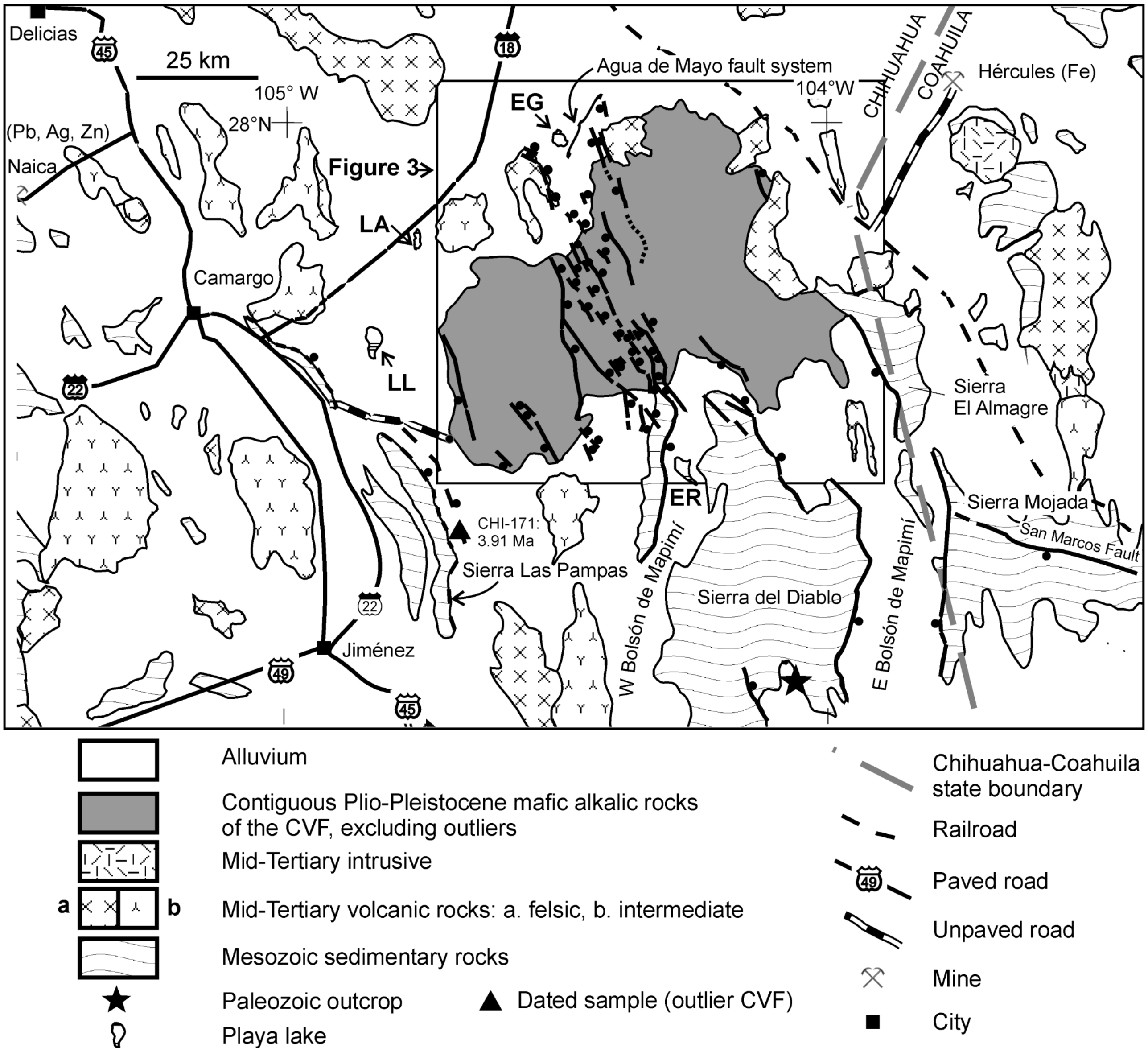

Figure 2. Regional setting of the Camargo volcanic field (CVF). Near the southern end of Sierra El Diablo are exposed Paleozoic volcanic rocks. The San Marcos fault, as documented by McKee et al. (1984, 1990), ends at the eastern branch of Bolsón de Mapimí. Playa lakes: LL—El Llano; EG—El Gigante; LA—Las Arenosas; ER—El Remolino.

tiary rocks. Regionally, Laramide folds near the volcanic field trend from north-northwest to west-northwest (Sociedad Geológica Mexicana, 1985; Tarango-Ontiveros, 1993). Tilted and faulted Eocene conglomerate and gravel are exposed adjacent to some of the folded limestone ranges (McKee et al., 1984, 1990; Bartolino, 1992). Subduction-related volcanic rocks (andesite-rhyolite) crop out extensively in the northeastern Camargo volcanic field (Figs. 2 and 3). These Tertiary volcanic rocks (K-Ar: 40–31 Ma; Smith, 1993; Smith et al., 1996) lie in the southernmost part of a 150-km-wide, east-northeast–trending belt of middle Cenozoic volcanic outcrops that extends from the Sierra Madre Occidental into west Texas (Fig. 1). Lavas of the Camargo volcanic field rest atop Cretaceous marine sedimentary rocks, middle Tertiary volcanic rocks, or, locally, gravel composed of fragments of limestone and volcanic rocks. An andesitic sill (Table 1: $^{40}Ar/^{39}Ar = 13.97 \pm 0.08$ Ma) that intruded gravel near Sierra Aguachile provides a minimum age for the Tertiary arc-related magmatism (Fig. 3).

The Camargo volcanic field overlaps an antithetic transfer zone between basin-and-range structures. South of the field, the Sierras San Francisco and El Diablo are bounded to the east by approximately north-striking, down-to-the-east normal faults (Fig. 3). These faults abruptly change strike to N30°W and project into the central Camargo volcanic field. North of the volcanic field and partly buried by its lavas, the Sierra Agua de Mayo is bounded by a N10°W, down-to-the-southwest, right-stepping, en echelon system of normal faults. The opposing Agua de Mayo and San Francisco–El Diablo fault systems meet beneath the central

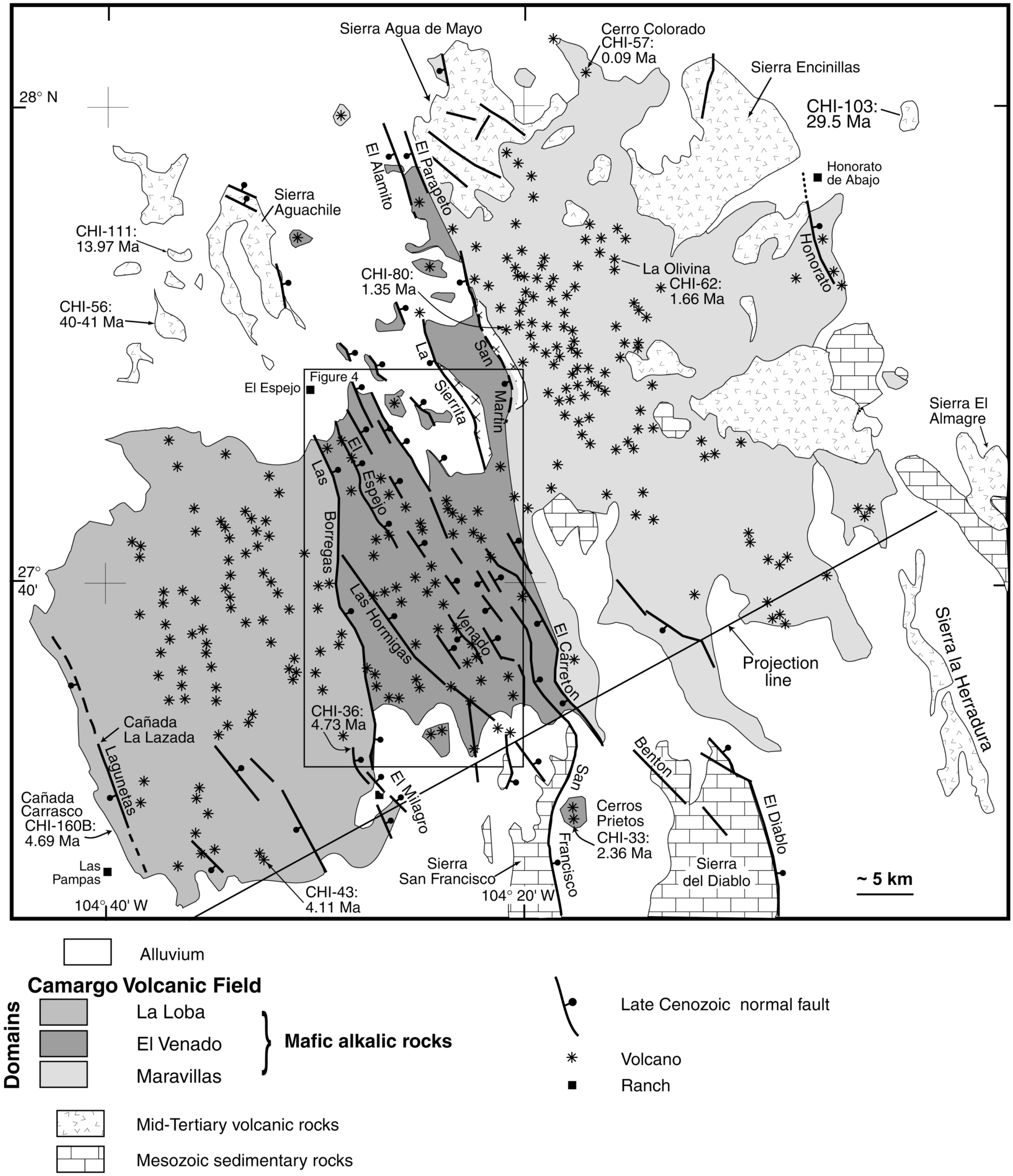

Figure 3. Generalized geologic map of the Camargo volcanic field. The box in the central part of the volcanic field shows the location of Figure 4.

TABLE 1. SUMMARY OF $^{40}Ar/^{39}Ar$ AGES OBTAINED FOR ROCKS OF THE CAMARGO VOLCANIC FIELD AND ITS SURROUNDINGS, AND MINIMUM VERTICAL SLIP RATES FOR FAULTS IN THE CENTRAL GRABEN OF THE CAMARGO VOLCANIC FIELD

Sample	Type	Latitude (N)	Longitude (W)	Age $\pm 2\sigma$ (Ma)	Δ age[†] (m.y.)	Throw[‡] (m)	Slip rate (mm/yr)[§]
Samples collected in the surroundings of the Camargo volcanic field							
CHI-56	Sill	27° 51.181′	104°37.260′	40 to 41[‡‡]			
CHI-103	Neck	27° 59.558′	104°01.529′	29.50 ± 0.12			
CHI-111	Sill	27° 55.350′	104°36.831′	13.97 ± 0.08			
Samples not related to faulting from the Camargo volcanic field							
CHI-160B	Lava[#]	27°33.278′	104°40.432′	4.69 ± 0.06			
CHI-43	Neck	27°29.089′	104°33.186′	4.11 ± 0.04			
CHI-171	Cone	27°23.189′	104°41.672′	3.91 ± 0.03			
CHI-84	Cone	27°45.766′	104°28.402′	2.27 ± 0.04			
CHI-33	Cone	27°30.635′	104°18.168′	2.36 ± 0.10			
CHI-80	Cone	27°51.248′	104°22.255′	1.35 ± 0.10			
CHI-62	Cone	27°53.743′	104°16.006′	1.66 ± 0.10			
CHI-57	Cone	28°02.182′	104°17.624′	0.09 ± 0.04			
El Milagro fault							
CHI-36	Pre-fault	27°33.914′	104°28.542′	4.73 ± 0.04			
CHI-37	Post-fault	27°34.161′	104°28.927′	3.05 ± 0.12	1.84	>50	>0.03
Las Borregas fault at Cerro Mojoneras							
CHI-92	Pre-fault	27°36.906′	104°28.356′	2.30 ± 0.06			
CHI-91A	Post-fault	27°36.803′	104°28.520′	2.35 ± 0.06	0.07	>50	>0.71
CHI-91B	Post-fault[#]	27°36.803′	104°28.520′	2.37 ± 0.04	0.03	>50	>1.67[††]
Las Borregas fault at Cerro Lamojino							
CHI-53	Post-fault	27°41.035′	104°29.514′	2.45 ± 0.10	See text	>40	See text[††]
CHI-54	Post-fault[#]	27°41.035′	104°29.514′	2.54 ± 0.06			
Las Hormigas fault							
CHI-93	Pre-fault	27°36.157′	104°24.543′	2.25 ± 0.04	0	>10	See text
CHI-94	Post-fault	27°36.229′	104°24.032′	2.37 ± 0.08			
Northern end of Las Borregas							
CHI-85	Pre-fault	27°46.251′	104°30.446′	2.94 ± 0.02			
CHI-87	Post-fault	27°45.756′	104°30.288′	2.45 ± 0.04	0.55	>90	>0.16
El Venado fault							
CHI-99	Pre-fault	27°37.123′	104°23.725′	2.24 ± 0.02			
CHI-98A	Post-fault	27°36.921′	104°23.501′	2.14 ± 0.22	0.34	>10	>0.03
El Espejo fault							
CHI-83	Pre-fault	27°46.049′	104°28.569′	2.19 ± 0.02			
CHI-82	Post-fault	27°45.992′	104°29.099′	2.18 ± 0.06	0.09	>10	>0.11

[†]See Table DR1.
[‡]Degraded scarp heights.
[§]See discussion in text.
[#]Age obtained from feldspar megacrysts.
[††]To calculate slip rates we used the age obtained from groundmass separates.
[‡‡]See Figure 5.

part of the Camargo volcanic field to produce the central graben.

GEOLOGIC OVERVIEW OF THE CAMARGO VOLCANIC FIELD

The Camargo volcanic field is the largest and most voluminous of the xenolith-bearing basaltic volcanic fields in the southern Basin and Range province (Fig. 1), and its relationship to late Cenozoic faulting is the most evident. The volcanic field is formed by >300 recognized vents and extensive lava fields, which cover an area of ~3000 km^2. As discussed in this paper, a rough estimate of the average thickness of the lava plateau is ~40 m, yielding an estimated lava volume of ~120 km^3.

Twenty-three new $^{40}Ar/^{39}Ar$ ages of volcanic rocks of the Camargo volcanic field range from 4.73 ± 0.04 Ma (CHI-36) to 0.09 ± 0.04 Ma (CHI- 57); all reported uncertainties are two standard deviations (2σ, Table 1). The best-known locality in the volcanic field is La Olivina, a cinder cone (Table 1: $^{40}Ar/^{39}Ar$ = 1.66 ± 0.10 Ma) where spinel lherzolite mantle xenoliths are abundant (Nimz et al., 1995). La Olivina also yields middle- to lower-crustal feldspathic granulites (Cameron et al., 1983, 1992; Nimz et al., 1986; Rudnick and Cameron, 1991) and two distinct types of subcrustal pyroxenites, one regarded as comagmatic with the host lavas and the other as comagmatic with the middle Tertiary basalts of the area (Nimz et al., 1993). Small (<3 cm) mantle and crustal xenoliths are also found throughout the Camargo volcanic field.

Ongoing faulting and block uplift in the volcanic field are evidenced by features commonly associated with these processes (Keller, 1986), such as offsets in alluvial fans, fanhead deposition near the apex of alluvial fans, flatirons, and abrupt low-sinuosity mountain fronts. Active extension in southern Chihuahua is also supported by the observed seismicity, together with the length, focal depth, and rupture complexity associated with the Parral earthquake (1928, M = 6.5), which are similar to the values that characterize events of comparable magnitude elsewhere in the Basin and Range province (Doser and Rodríguez, 1992).

DOMAINS OF THE CAMARGO VOLCANIC FIELD

The lava plateau of the Camargo volcanic field is cut by a central graben, which divides the field into three large volcano-tectonic domains. The domains are bounded by normal faults or fault systems and characterized by different ages of volcanism and fault density (Fig. 3). We term these domains La Loba (southwestern), El Venado (central), and Maravillas (northeastern).

La Loba Domain

The southwestern part of the Camargo volcanic field is a relatively unfaulted lava plain with abundant remnants of deeply eroded cinder cones. Consequent streams, roughly perpendicular to the abrupt, southwestern boundary of the lava plain, incise deep canyons where thick lava-flow stacks are exposed. Vent locations in the southwestern part of the domain are marked by low rounded hills without vestiges of craters. The centers of these scoria mounds are commonly marked by small plug-like lava necks with near-vertical flow foliation and platy joints. Randomly oriented dikes radiate from these necks. Volcanic necks also occur in the eastern part of the La Loba domain, as well as some breached volcanoes characterized by broad shallow craters with gentle inner walls. The outer slopes of the cones commonly exceed 33° and may be as steep as 43°. These unusually steep slopes are products of erosion, which exposes resistant beds of volcanic agglutinate.

La Loba domain is bounded on the west and east by normal faults. It abruptly ends on the west along the Lagunetas fault (Fig. 3). The fault trace between Cañada La Lazada and Cañada Carrasco cuts and displaces the lava flows (Fig. 3). Near the northern and southern ends of the Lagunetas fault, the fault trace is covered by distal lava flows from younger La Loba volcanoes to the east. Therefore, activity along the Lagunetas fault probably ended before the onset of volcanism and faulting in the younger Venado domain to the east. The Las

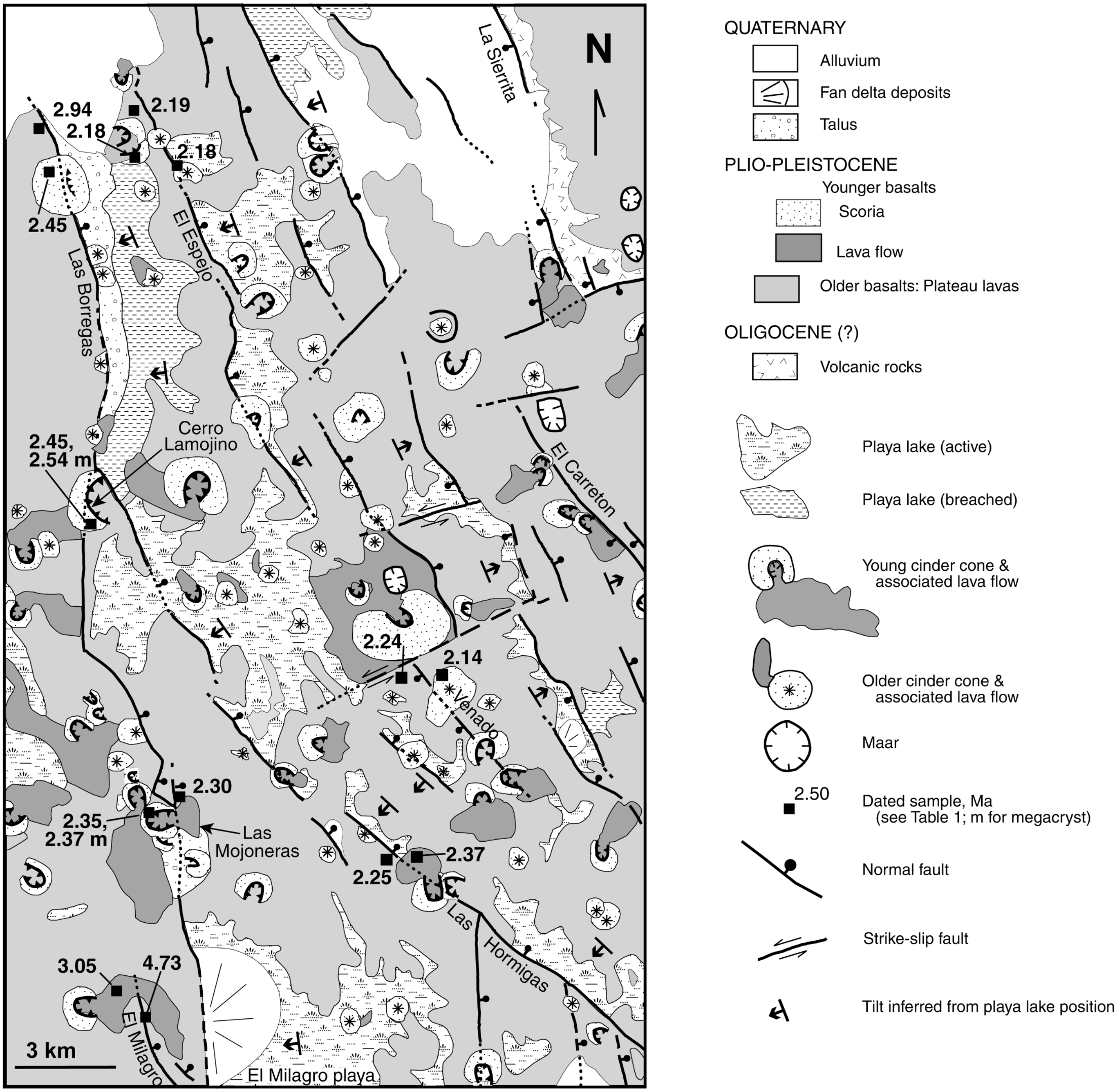

Figure 4. Geologic map of the El Venado domain.

Borregas and El Milagro fault systems separate the La Loba and El Venado domains. The fact that the trace of the Las Borregas system is locally covered by younger volcanoes (e.g., Cerros Lamojino and Las Mojoneras: Fig. 4; Cetenal, 1974) indicates that it acted as a magmatic conduit. The elliptical shape of Cerro Lamojino, having its long axis parallel to the fault, suggests that it was formed by a series of eruptions along the structure. Contact relationships around Cerro Mojoneras are complex and are best explained by several successive pulses of faulting and volcanism.

El Venado Domain

The central El Venado domain is characterized by numerous normal faults with scarps up to ~100 m high and small intervening playa lakes. Approximately one half of the vents are low hills with necks and radial dikes, and the rest are younger breached cones with distinct craters (Fig. 4). Short individual lava flows that caused partial collapse of the cones by rafting are common. These younger volcanic features are scattered over an older lava plain. Alignment of vents along faults indicates that the faults acted as magma conduits; younger cinder cones cover some fault traces. The en echelon Agua de Mayo fault system—formed by El Alamito, El Parapeto, La Sierrita, San Martín, and El Carretón faults (Figs. 2–3)—marks the eastern limit of the domain. Aerial-photographic analysis and field observations indicate that the north-northwest–striking, down-to-the-southwest Agua de Mayo fault system (Fig. 2) gradually transforms southward, beneath the Camargo volcanic field, into the northwest-striking, down-to-the-northeast San Francisco fault. Farther south this structure abruptly changes to a north trend and has a larger displacement than shown where it cuts the volcanic field. Thus, displacement on both the Agua de Mayo system from the north and the San Francisco fault from the south decreases as they approach the volcanic field. However, Mesozoic sedimentary rocks along the San Francisco fault and middle Tertiary volcanic rocks along the Agua de Mayo system show the greatest displacement, indicating significant pre–Camargo volcanic field motion along these structures. Active uplift of the east-central Sierra San Francisco is suggested by flatirons, low sinuosity of the mountain front, and fanhead deposition at the apex of alluvial fans. Occurrence of a small, internally drained basin and a playa lake (Laguna El Remolino: Fig. 2) immediately east of the mountain front and south of Cerros Prietos indicates southwestward tilting of the hanging-wall block.

In the central graben of the El Venado domain, the timing of movement along different faults can be bracketed by $^{40}Ar/^{39}Ar$ dating of associated lava flows, as discussed subsequently. Relationships are clearest for faults with relatively small throws, where we could collect and date a lava flow cut by the fault and another draping the fault. Such cases are discussed for the faults El Espejo, El Milagro, and El Venado (Fig. 4). Extensive talus deposits that bury the fault traces hinder detailed interpretation of the geologic history at many localities. It can also be extremely difficult to establish whether a cinder cone was partly destroyed by a younger faulting episode or whether it erupted very close to an older fault scarp, built part of its cone above the footwall of the structure, and later was destroyed by mass-wasting and/or fluvial erosion.

Closed basins are common in the Camargo volcanic field region. Regional normal faulting associated with late Cenozoic basin-and-range extension controlled the locations of relatively large playa lakes such as El Gigante, Las Arenosas, El Llano, and El Remolino (Fig. 2). Internally drained basins are common in the El Venado domain, and the distribution of lakes and their association with fault scarps indicate that they were caused by slight tilting associated with normal faulting (Fig. 4). The largest basin in the El Venado domain is occupied by the El Milagro playa lake, which contains a well-developed fan delta near the trace of the Las Borregas and El Milagro fault systems (Fig. 4). Slight tilting, coupled with the modest observed displacement in the central graben of the Camargo volcanic field, indicates that Pliocene–Pleistocene extension in the area is low.

Maravillas Domain

The northeastern Camargo volcanic field domain, named Maravillas, is relatively unfaulted and covered by extensive lava flows; vents are particularly abundant west of La Olivina (Fig. 3). Morphologically, the vast majority of the Maravillas vents are breached cones characterized by distinct craters with relatively steep inner walls and outer cone slopes as steep as 22°. These features are interpreted as indicating only moderate degrees of erosion, lower than that found in the other two domains, and consistent with young ^{40}Ar-^{39}Ar ages discussed in the next section. Cones with steep outer slopes (>33°) and exposed agglutinate beds are rare compared with the other domains, and necks are absent, except at the northeastern edge of the Maravillas domain; however, we determined that these necks are middle Tertiary in age (29.5 Ma). The presence of isolated outcrops of such older rocks, partially to completely surrounded by mafic lavas of the Camargo volcanic field, indicates that the Pliocene topography of the area was irregular. The northeastern and southeastern boundaries of the Maravillas domain are very irregular because relatively voluminous lava flows moved down prevolcanic stream beds and formed elongated lobes. Near the northeastern end of the domain, the Honorato fault (Fig. 3) cuts and displaces alluvial-fan deposits and Pleistocene lava flows of the Camargo volcanic field and is partly buried by younger alluvial deposits. Compared with other faults at the boundaries between the Camargo volcanic field domains, the Honorato fault has small displacement, just a few meters, but its trace is quite clear.

AGE OF VOLCANISM AND FAULTING

In total, 26 new $^{40}Ar/^{39}Ar$ ages were determined at Berkeley Geochronology Center (Tables 1 and DR-1[1]; Figs. 5–7) by using the analytical methods described by Sharp et al. (1996). Materials dated included 20 groundmass separates and 3 feldspar megacrysts from the Camargo volcanic field, plus 3 groundmass separates from mafic volcanic rocks older than the Camargo volcanic field. Our goals were to (1) establish the duration of activity for the Camargo volcanic field by dating vents with different estimated geomorphologic ages (Noyola-Medrano, 1995), (2) evaluate whether feldspar megacrysts, which may be xenocrystic (e.g., Luhr et al., 1995a), can provide reliable ages for their host lavas, (3) determine the ages of other mafic volcanic rocks near the Camargo volcanic field, and (4) set limits on the vertical slip rates for some of the faults in the central graben.

All samples gave readily interpretable results. Plateau and inverse isochron ages agree within analytical uncertainties for all but one very young sample. Sample CHI-57 gave imprecise plateau, 0.50 ± 0.30 Ma, and isochron ages, 0.09 ± 0.04 Ma, not surprising given its very young age. We choose the isochron age because the isochron data indicate only a small amount of excess argon. The quality of the isochron result suggests that this is the most accurate reflection of true geologic age.

Northeastward Migration of Volcanism

Sample ages for the Camargo volcanic field range between 4.73 ± 0.04 (CHI-36) and 0.09 ± 0.04 Ma (CHI-57, Table 1) and decrease from southwest to northeast (Figs. 2–4). The four oldest samples are from the southwestern part of the volcanic field, either within or adjacent to the La Loba domain. CHI-171 (3.91 ± 0.03 Ma) is from an outlier vent located ~15 km south-southwest of the southwestern corner of the contiguous Camargo volcanic field (Fig. 2). CHI-160B (4.69 ± 0.06 Ma) is a feldspar megacryst ($Ca_{43}Na_{53}K_4$) from a lava flow exposed at the base of the La Loba volcanic sequence in Cañada Carrasco (Fig. 3). CHI-36 (4.73 ± 0.04 Ma) came from a lava flow at the base of the sequence that is cut by the El Milagro fault (Figs. 3–4). Vent locations for these two samples are unknown. CHI-43 (4.11 ± 0.04 Ma) is from a volcanic neck near the southwest part of the La Loba domain (Fig. 3).

The youngest rocks in the dated set are from the Maravillas domain, in the northeast

[1]GSA Data Repository item 2003033, $^{40}Ar/^{39}Ar$ analytical data, is available on the Web at http://www.geosociety.org/pubs/ft2003.htm. Requests may also be sent to editing@geosociety.org.

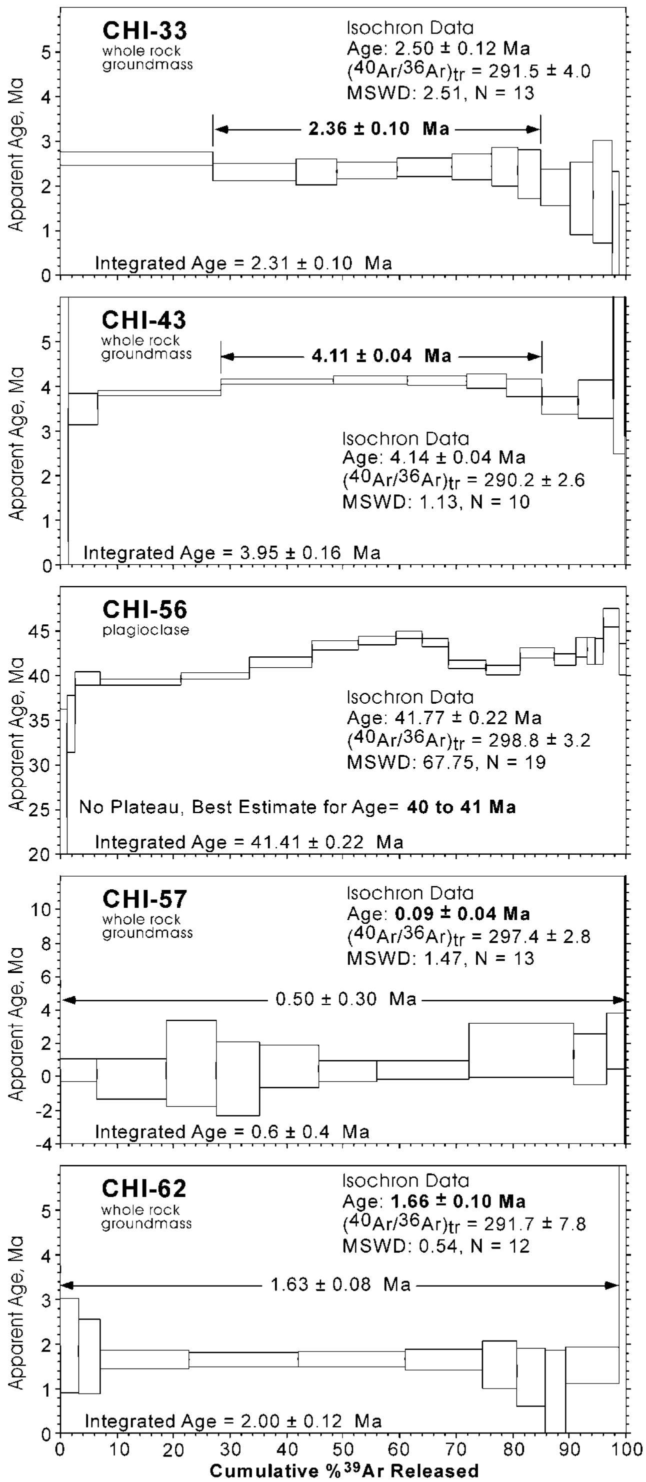

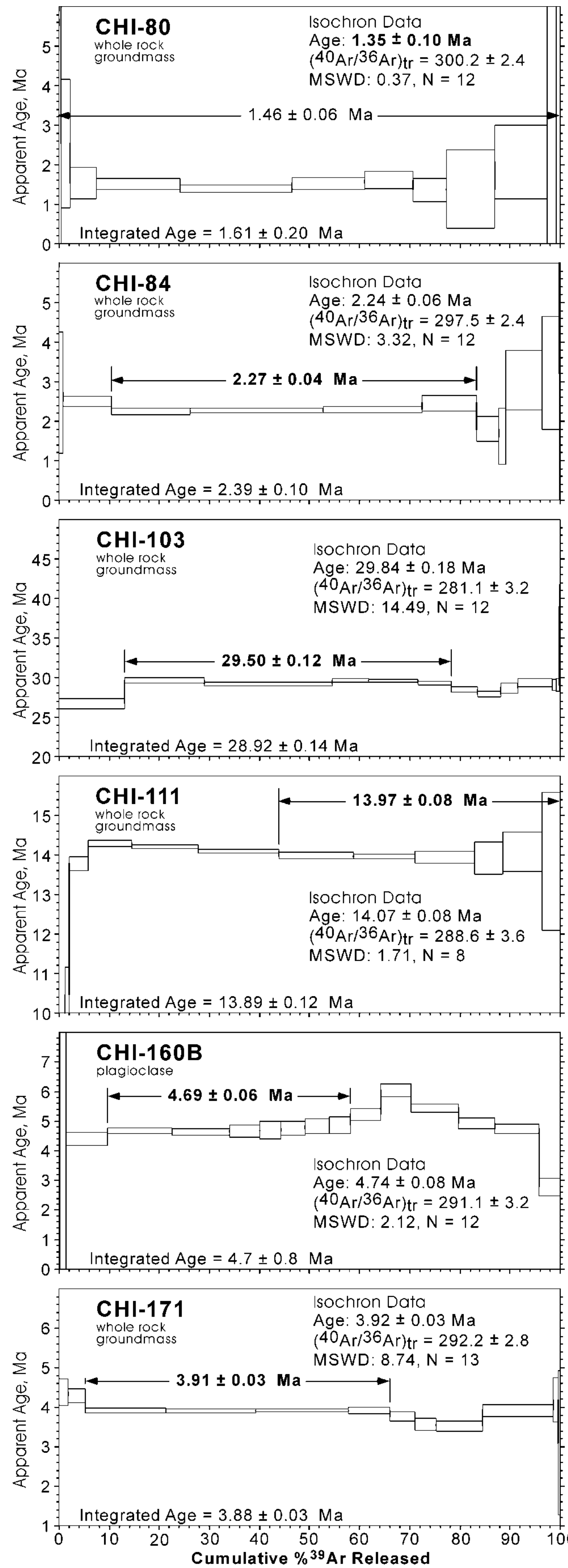

Figure 5. $^{40}Ar/^{39}Ar$ **incremental heating spectra and inverse isochron data for samples unrelated to faulting. Uncertainties for all ages and ratios are ±2 standard deviations. Vertical height of each increment in spectra is 2 standard deviations. The preferred age for each sample is in boldface type. Subscript tr denotes the initial or "trapped" component of the** $^{40}Ar/^{36}Ar$ **ratio.**

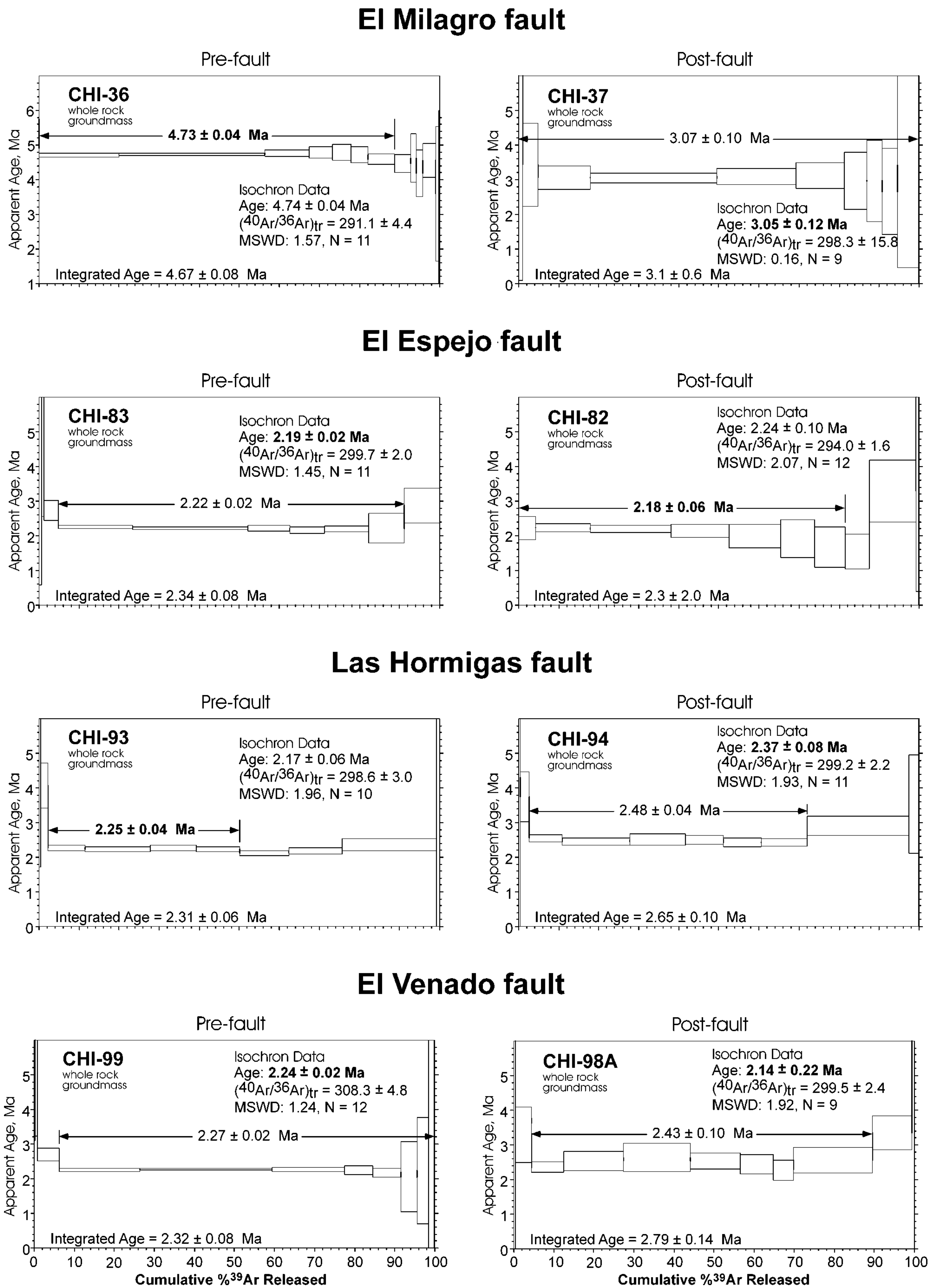
El Milagro fault
Pre-fault
CHI-36
whole rock groundmass
4.73 ± 0.04 Ma
Isochron Data
Age: 4.74 ± 0.04 Ma
(40Ar/36Ar)tr = 291.1 ± 4.4
MSWD: 1.57, N = 11
Integrated Age = 4.67 ± 0.08 Ma
Apparent Age, Ma
Post-fault
CHI-37
whole rock groundmass
3.07 ± 0.10 Ma
Isochron Data
Age: 3.05 ± 0.12 Ma
(40Ar/36Ar)tr = 298.3 ± 15.8
MSWD: 0.16, N = 9
Integrated Age = 3.1 ± 0.6 Ma
El Espejo fault
Pre-fault
CHI-83
whole rock groundmass
Isochron Data
Age: 2.19 ± 0.02 Ma
(40Ar/36Ar)tr = 299.7 ± 2.0
MSWD: 1.45, N = 11
2.22 ± 0.02 Ma
Integrated Age = 2.34 ± 0.08 Ma
Post-fault
CHI-82
whole rock groundmass
Isochron Data
Age: 2.24 ± 0.10 Ma
(40Ar/36Ar)tr = 294.0 ± 1.6
MSWD: 2.07, N = 12
2.18 ± 0.06 Ma
Integrated Age = 2.3 ± 2.0 Ma
Las Hormigas fault
Pre-fault
CHI-93
whole rock groundmass
Isochron Data
Age: 2.17 ± 0.06 Ma
(40Ar/36Ar)tr = 298.6 ± 3.0
MSWD: 1.96, N = 10
2.25 ± 0.04 Ma
Integrated Age = 2.31 ± 0.06 Ma
Post-fault
CHI-94
whole rock groundmass
Isochron Data
Age: 2.37 ± 0.08 Ma
(40Ar/36Ar)tr = 299.2 ± 2.2
MSWD: 1.93, N = 11
2.48 ± 0.04 Ma
Integrated Age = 2.65 ± 0.10 Ma
El Venado fault
Pre-fault
CHI-99
whole rock groundmass
Isochron Data
Age: 2.24 ± 0.02 Ma
(40Ar/36Ar)tr = 308.3 ± 4.8
MSWD: 1.24, N = 12
2.27 ± 0.02 Ma
Integrated Age = 2.32 ± 0.08 Ma
Cumulative %39Ar Released
Post-fault
CHI-98A
whole rock groundmass
Isochron Data
Age: 2.14 ± 0.22 Ma
(40Ar/36Ar)tr = 299.5 ± 2.4
MSWD: 1.92, N = 9
2.43 ± 0.10 Ma
Integrated Age = 2.79 ± 0.14 Ma
Cumulative %39Ar Released

part of the Camargo volcanic field (Fig. 3). These include a youthful-looking lava flow with vestigial pahoehoe ropes from the moderately eroded cinder cone Cerro Colorado (CHI-57, 0.09 ± 0.04 Ma), a lava flow that overlies the San Martín fault near the Cañón Obscuro Ranch (CHI-80, 1.35 ± 0.10 Ma), and a bomb from La Olivina (CHI-62, 1.66 ± 0.10 Ma).

All 15 dated groundmass samples and feldspars of intermediate age (2.94 ± 0.02 [CHI-85] to 2.14 ± 0.22 Ma [CHI-98A]) come from the central domain, El Venado, or just to its west (Figs. 3 and 4). The 2.36 ± 0.10 Ma age of Cerros Prietos (CHI-33), an isolated cinder-cone complex south of the El Venado domain, agrees with ages of rocks within the domain (Fig. 3).

The $^{40}Ar/^{39}Ar$ ages demonstrate that volcanism migrated northeastward (Fig. 8B) at an average rate of ~15 mm/yr. This estimate uses only samples from identifiable vents (Fig. 8A), thereby excluding lava-plain samples whose source-vent locations are unknown and potentially distant from the sampling sites. Vent ages were projected onto a N60°E-trending line (Fig. 3), which is approximately perpendicular to the Pliocene–Pleistocene tectonic grain defined by the trends of synvolcanic normal fault scarps. The total distance (~60 km) between the oldest vent in the southwest part of the field and the youngest volcano was divided by the life span of the field (~4 m.y.), inferred from the $^{40}Ar/^{39}Ar$ ages of known vents. It is not possible from the available data to establish whether the shift in volcanic activity was continuous or episodic. Ages shown in Figure 8A appear to cluster in intervals older than 4, approximately 3, 2.5–2.2, 1.6–1.3, and 0.09 Ma. This clustering may reflect an episodic phenomenon or incomplete sampling. Furthermore, although the oldest volcanoes are generally in the southwest part of the field and the youngest in the northeast, as seen in Figure 4, there is significant overlap between the areas with morphologically old and intermediate-age volcanoes. Migration of alkali olivine basalt vents has also been documented in the San Francisco volcanic field of Arizona (29 ± 3 mm/yr toward 93° ± 5°; Tanaka et al., 1986) and the Springerville field of Arizona (29 ± 11 mm/yr toward 93° ± 22°; Condit et al., 1989b). These displacements have been interpreted as the result of migration of the North American plate over fixed mantle hotspots.

Eruption Rate

A conservative estimate of the total lava volume of the Camargo volcanic field is ~120 km^3, based on an area of ~3000 km^2 and a roughly estimated average thickness of 40 m for the contiguous field. Polymictic gravels are exposed beneath lava flows in several places around the border of the volcanic plateau and along the Las Borregas and El Caretón fault scarps (Fig. 4). Our local estimates of the thickness of the volcanic pile above the gravels vary between 10 and 50 m. At the western edge of the Camargo volcanic field, in the barrancas (gullies) that drain into the El Llano playa (Fig. 2), it is evident that lava stacks may locally reach 100 m in areas with relatively high vent density, such as the central part of the La Loba and Maravillas domains. Therefore, we infer that an average of 40 m for the lava plateau is conservative. Furthermore, the fact that most volcanoes in the La Loba and El Venado domains are moderately to deeply eroded, as shown by the geomorphologic analysis performed by Noyola-Medrano (1995), makes a more precise estimate very difficult.

If the ages obtained for the oldest (CHI-36, 4.73 ± 0.04 Ma) and youngest (CHI-57, 0.09 ± 0.04 Ma) samples represent the life span of the volcanic field (4.72 Ma at the 2σ level), the long-term eruption rate is ~0.026 km^3/k.y. This is similar to eruption rates reported for other intraplate continental volcanic fields, such as the Ocate (New Mexico), Lunar Crater (Nevada), and Durango (México) fields (Table 2), but considerably lower than rates calculated for the intraplate Springerville field and the subduction-related Michoacán-Guanajuato volcanic field. All these are dwarfed by eruption rates for the world's largest intraplate, oceanic volcanoes, such as Kilauea and Mauna Loa.

Age of Feldspar Megacrysts

Feldspar megacrysts are common at many localities in the Camargo volcanic field, in other late Cenozoic mafic alkalic volcanic fields in the Basin and Range province, and in mafic alkalic volcanic rocks from continental rift zones worldwide (e.g., Binns, 1969; Irving, 1974; Aspen et al., 1990). These inclusions range in size from a few millimeters to several centimeters and are either xenocrystic (foreign) or cognate with the host magma. Megacrysts are commonly released from the lava or tephra deposits by differential weathering and can easily be collected as unaltered crystals on the surface of the flows. Regardless of their origin, if these feldspar megacrysts were at a temperature in excess of the Ar blocking temperature prior to eruption, or completely degassed during transport, they could be used directly to date the eruption.

Feldspar megacrysts CHI-91B ($An_{22}Ab_{72}Or_6$) and CHI-54 ($An_{27}Ab_{67}Or_6$) were collected at the same sites as volcanic rocks CHI-91A and CHI-53, respectively, whose groundmasses were also dated. In both cases the megacryst and groundmass ages are indistinguishable at the 2σ level (Table 1). Although some workers have reported problems in obtaining reliable $^{40}Ar/^{39}Ar$ ages from feldspar (e.g., Foland, 1974; Harrison, 1990), our results indicate that feldspar megacrysts can yield reliable eruption ages for host volcanic rocks.

Ages of Other Volcanic Rocks near the Camargo Volcanic Field

The three older dated volcanic rocks near the Camargo volcanic field (Fig. 3) are all calc-alkalic and compositionally distinct from the mafic alkalic rocks of the Camargo volcanic field. Two of these are from the northwest margin of the volcanic field. CHI-56 (41–40 Ma) is a hypersthene-normative basalt from the thick, columnar-jointed Cerro Prieto sill (Smith, 1993). This age is similar to those reported by Smith et al. (1996) for the oldest middle Tertiary volcanic rocks in this region. CHI-111 (13.97 ± 0.08 Ma) is a quartz-normative trachyandesite, collected from another columnar-jointed sill (Smith, 1993) ~6 km to the north-northeast. This sill is ~20 m thick and overlies ~15 m of poorly sorted, poorly consolidated, coarse-grained, polymictic sandstones that are partly conglomeratic. These sediments appear to correlate with the gravels that elsewhere underlie the mafic alkalic rocks of the Camargo volcanic field, indicating that the gravels are older than 14 Ma. The third of the older dated rocks is from the northeast margin of the Camargo volcanic field; CHI-103 (29.50 ± 0.12 Ma) is a quartz-normative trachybasalt, collected from an apparent volcanic neck northeast of Honorato de Abajo (Fig. 3). Its age is slightly younger than ages obtained by Smith et al. (1996) for the

Figure 6. $^{40}Ar/^{39}Ar$ incremental heating spectra and inverse isochron data for sample pairs related to faulting. Left-column samples are determined to be prefaulting. Right-column samples are corresponding samples determined to be postfaulting. See notes for Figure 5.

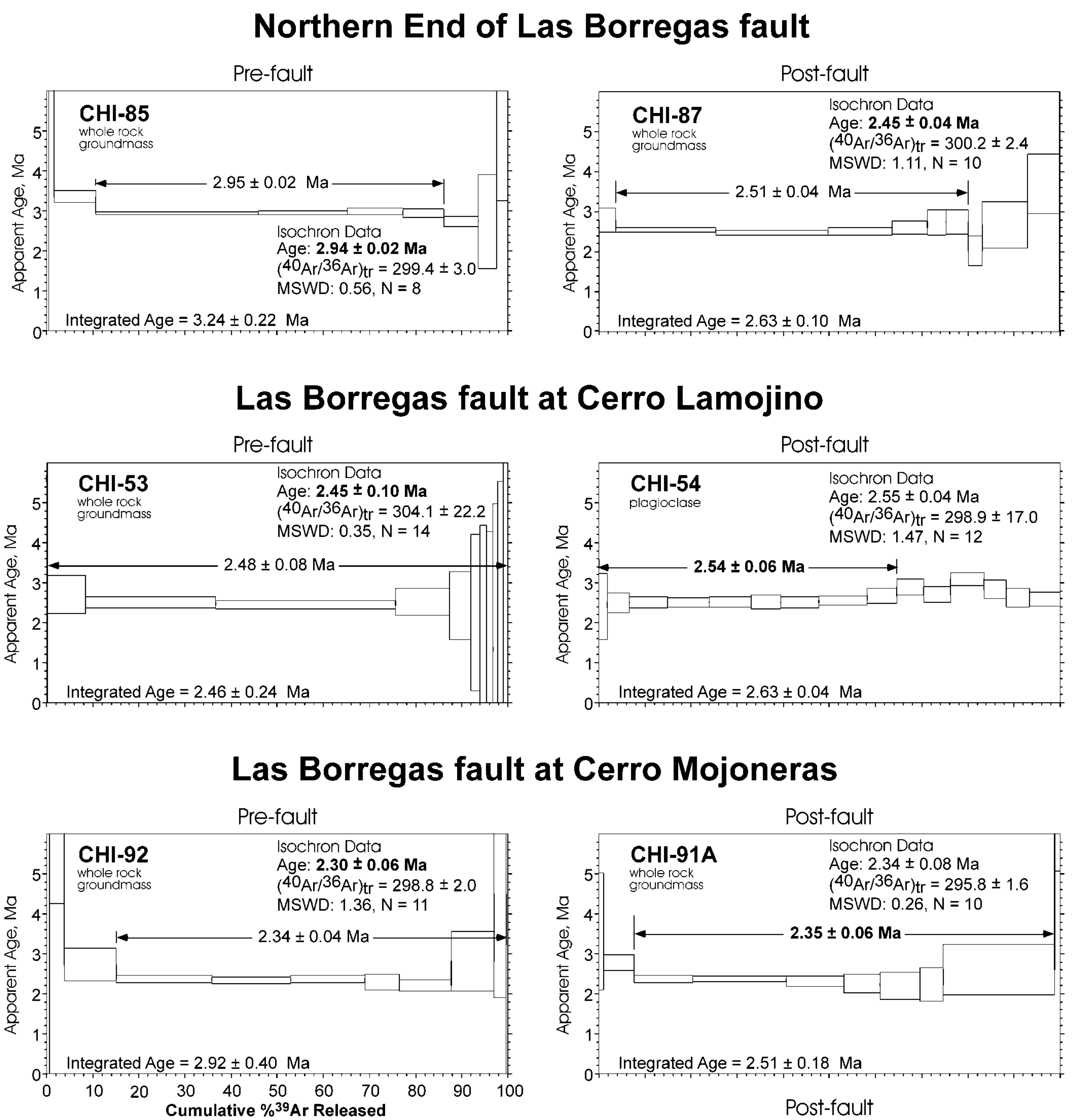

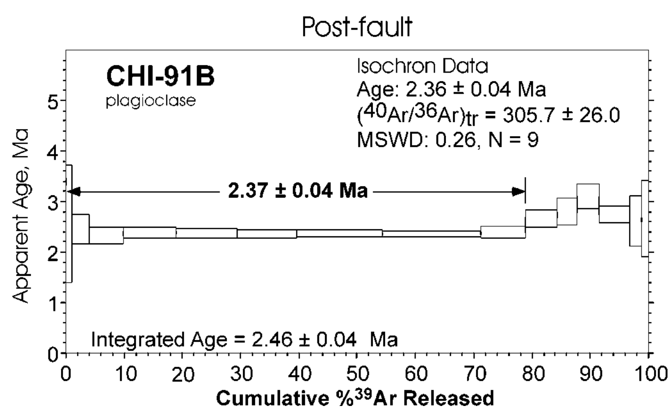

Figure 7. $^{40}Ar/^{39}Ar$ incremental heating spectra and inverse isochron data for sample pairs related to movement on the Las Borregas fault. Left-column samples are determined to be prefaulting. Right-column samples are corresponding samples determined to be postfaulting. See notes for Figure 5.

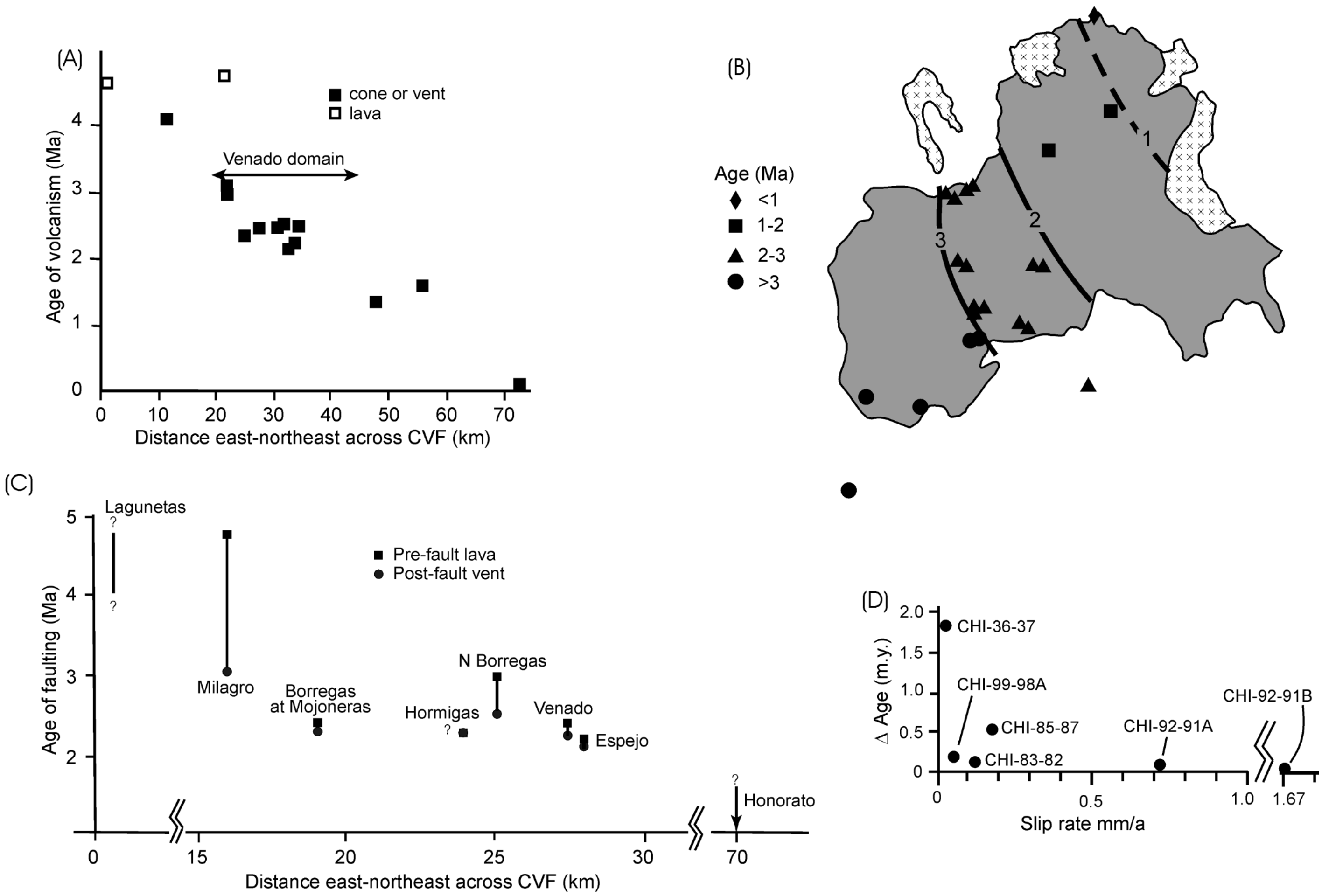

Figure 8. Summary of $^{40}Ar/^{39}Ar$ results. (A) Ages of dated volcanoes (excluding outliers) projected onto a N60°E-trending line. (B) Isochron map of the Camargo volcanic field using the $^{40}Ar/^{39}Ar$ results with intervals of 1, 2, and 3 Ma. (C) Ages of dated faults projected onto a N60°E-trending line. The Lagunetas and Honorato faults were not dated and are positioned schematically on the basis of field relationships that indicate their relative ages with respect to faults in the central graben. (D) Plot of elapsed time between delimiting ages vs. minimum vertical slip rates in the central part of the Camargo volcanic field.

middle Tertiary Agua de Mayo volcanic group in this region.

Timing of Faulting

Our new $^{40}Ar/^{39}Ar$ ages also set limits on the timing of faulting in the Camargo volcanic field and provide some of the first vertical slip rates for faults in the Mexican part of the Basin and Range province. Plotting the ages of dated faults along the N60°E-trending line (Fig. 8C) suggests that the faulting, or at least the cessation of faulting, may also have migrated from southwest to northeast. The observation that the Lagunetas fault cuts some La Loba lavas but is buried by others erupted in the eastern part of the domain indicates that the fault last slipped before volcanism and faulting in the Venado domain commenced; thus the Lagunetas fault was active between 4.7 and 3.05 Ma. The easternmost structure of the La Loba domain (El Milagro) is older than four faults from the Venado domain. The latter domain appears to have formed during a relatively short (~0.8 m.y.) period of synchronous volcanism and faulting. The Honorato fault, located in the northeast part of the field, was not dated in this study, but it cuts alluvium and lavas younger than those in the Venado region and thus appears to be among the youngest faults in the Camargo volcanic field.

CALCULATION OF SLIP RATES FOR NORMAL FAULTS IN THE CAMARGO VOLCANIC FIELD

The $^{40}Ar/^{39}Ar$ ages (Figs. 5–7) were used to calculate minimum vertical slip rates for several faults of the Camargo volcanic field. Following the work of McCalpin (1995), we assumed that the degraded scarp heights are equivalent to the minimum vertical component, because the top of the downthrown block is invariably buried under alluvium, lake beds, and/or talus deposits of unknown thickness. Additional uncertainties in the estimated slip rates arise from (1) errors in estimating the fault-scarp heights from topographic maps with 10 m contour intervals, (2) reported uncertainties in the isotopic ages of the two samples used to bracket the age of the fault (in order to calculate minimum slip rates we used maximum age differences at the 2σ level; Table 1), and (3) the assumption that total strain accumulated over the entire time period limited by the dated samples.

Three different types of sample pairs are

TABLE 2. CALCULATED ERUPTION RATES FOR THE CVF AND OTHER VOLCANIC FIELDS

Locality	Duration (Ma)	Area (km)	Volume (km^3)	Rate (km^3/ka)	Rate/Area (km^3/ka-km)
Camargo volcanic field[†]	4.64	3000	120	0.026	8.6E–6
Servilleta basalt[‡]	1.0		200	0.2	
Ocate volcanic field[§]					
Pulse 1	2.6	95	0.9	0.002	2.1E–5
Pulse 2	0.8	420	31	0.04	9.5E–5
Pulse 3	0.2	320	23	0.12	3.8E–4
Pulse 4	0.2	360	28	0.14	3.9E–4
Pulse 5	0.6	185	4.0	0.007	3.8E–5
Total	4.4	1380	89.9	0.02	1.5E–5
Springerville volcanic field[#]	1.8	3000	300	0.17	5.6E–5
Durango volcanic field	1.64[‡‡]	2200	33[††]	0.02	9.1E–6
Michoacán-Guanajuato volcanic field[§§]	0.04	15,000	31	0.8	5.3E–5
Lunar Crater volcanic field[##]	5.7		100	0.018	
Mount Etna[##]	0.000439		3.6	8.2	
Kilauea[##]	0.000185		3.3	17.8	
Mauna Loa[##]	0.5		42,500	85	

†This paper.
‡Dungan et al. (1986).
§Nielson and Dungan (1985).
#Condit et al. (1989a).
††Smith (1989).
‡‡McIntosh, W.C. (written comm., 1998).
§§Hasenaka and Carmichael (1985).
##Crisp (1984).

recognized (Table 1). For the first type, the two samples have ages that are well resolvable by ^{40}Ar/^{39}Ar dating; these samples are associated with the El Milagro, El Venado, and El Espejo faults, and the northern end of the Las Borregas fault (Table DR-1). For these faults, minimum heights divided by the maximum age differences yield minimum slip rates averaged over those time intervals. The vertical displacement for the Borregas fault is $>$90 m, corresponding to a slip rate of $>$0.16 mm/yr. The minimum throw for the El Milagro fault is 50 m, corresponding to an estimated slip rate of $>$0.03 mm/yr. In the case of the El Venado fault, the maximum age difference between the dated samples is 0.34 m.y., and the scarp height of $>$10 m yields a slip rate of $>$0.03 mm/yr. For the El Espejo fault, the maximum age difference between CHI-83 and CHI-84 is 0.09 m.y., and the scarp of 10 m gives a slip rate of $>$0.11 mm/yr.

For the second type of sample pairs, relevant to two different points along the same fault scarp (Las Borregas fault at Cerro Lamojino and at Cerro Mojoneras, Fig. 4), the ^{40}Ar/^{39}Ar ages overlap at the 2σ level. Slip-rate calculations can be still made. In the case of the Las Borregas fault at Cerro Mojoneras, the maximum age difference between CHI-92 and CHI-91A at the 2σ level is $[(2.30 + 0.06) \times 10^6 \text{ yr}] - [(2.35 - 0.06) \times 10^6 \text{ yr}] = 0.07 \times 10^6$ yr. Thus, dividing the minimum scarp height ($\sim$50 m) by this maximum age difference yields a slip rate of $>$0.71 mm/yr. Treating the pair CHI-92 and CHI-91B in the same way, a slip rate of $>$1.67 mm/yr is obtained.

The third type is represented by only one pair of samples collected on the Las Hormigas fault (Figs. 4–5; location in Fig. 3), where the median value of the closely similar ages is nonetheless the reverse of what was expected from field relationships (Fig. 8C), and the maximum age difference at the 2σ level is zero (Table DR-1). It is clearly not possible to estimate the slip rate from these data.

The implication of the ages for the second and third types of sample pairs is that the two bracketing eruptions and the intervening faulting occurred in very narrow time intervals. Therefore, these slip rates cannot be extrapolated to the regional context, and certainly they are not representative of long-term deformation.

A plot of the age differences for the sample pairs versus the minimum slip rates (Fig. 8D) shows that the average slip rate decreases dramatically as the age difference increases. Probably the high values of 0.71–1.67 mm/yr obtained for the Las Borregas fault at Cerro Mojoneras are short-term rates operative during periods of active faulting. The larger age differences between samples for the other faults are somewhat arbitrary, dictated as they are by the age of the uppermost plateau lava at that site, which probably had no direct relationship to the age of the faulting, and by the fact that displacement probably occurred during rapid clusters of paleoearthquakes separated by longer aseismic intervals (McCalpin, 1995). Independence of the lava-plain age from the age of faulting can be illustrated if slip rates of the Las Borregas fault are computed with samples CHI-53, CHI-85, and CHI-36. Sample CHI-53 was collected at Cerro Lamojino, a cinder cone that drapes the Las Borregas fault (Fig. 4). CHI-85 and CHI–36 are both samples of the lava plain exposed in the high scarps of the Las Borregas and El Milagro fault systems. Bracketing the age of the Las Borregas fault with samples CHI-53 and CHI-85 and considering a minimum throw of 40 m yields a minimum slip rate of $\sim$0.07 mm/yr. Calculating the time interval from the pair CHI-53 and CHI-36 by using the same 40 m throw yields a minimum slip rate of only $\sim$0.02 mm/yr, which is three times lower.

DISCUSSION

Faulting, Volcanism, and Regional Stress

Basaltic magma erupted as scoria cones and lava flows along active faults in the Camargo volcanic field (e.g., Fig. 4) because dikes abandon vertical ascent paths perpendicular to the least principal stress direction (σ_3) in favor of more energy-efficient paths along preexisting joints or faults (Conway et al., 1997). The orientation of a fault relative to σ_3 plays a key role in determining whether a fault zone is likely to dilate in response to dike injection (Connor and Conway, 2000). Given the synchronous nature of faulting and volcanism, most of the active normal faults in the Camargo volcanic field, especially in the El Venado domain, were perpendicular to σ_3 and were able to provide low-energy pathways for ascending dikes.

Parsons and Thompson (1991) suggested that the topography related to normal faulting is suppressed near volcanic fields because stress is accommodated by dilation of the crust during dike injection rather than by fault slip. This mechanism can explain much of the variation in structure of volcanic fields. For example, cinder-cone alignments are common in low-volume, low-density volcanic fields (e.g., Big Pine, California). In larger-volume basaltic fields, like the Springerville (Condit and Connor, 1996) and Michoacán-Guanajuato fields (Connor, 1990), mapped faults are rare, and cinder-cone alignments are less pervasive. In the Big Pine case, rates of dike injection were not sufficient to fully accommodate crustal stress. As a result, faults continued to slip, and dikes tended to parallel or inject into these faults. In contrast, rates of dike injection were sufficient to completely accommodate regional tectonic stresses within the larger Springerville and Michoacán-Guanajuato volcanic fields. This interpretation is also consistent with the antithetical spatial relationship between faults and plutons documented by

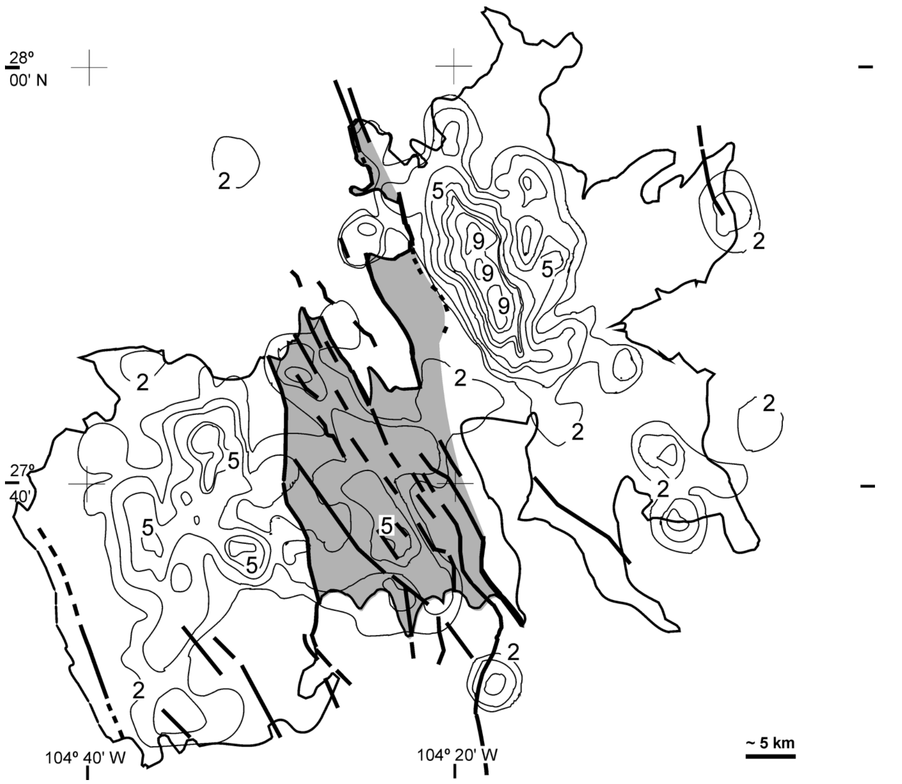

Figure 9. Vent and fault distributions in the Camargo volcanic field. Contour lines are vent densities obtained as follows: The number of vents around each volcano was counted in a circular area of 25 km². These values were used in the contouring process. The line that represents one volcano is not shown. Shaded area represents the El Venado domain, as shown in Figure 4. Heavy black lines are normal faults cutting the lava fields.

Paterson and Schmidt (1999) and Schmidt and Paterson (2000).

Regionally, volcanism in the Camargo volcanic field may account for the decreases in displacement along the San Francisco and Agua de Mayo faults as they approach the volcanic field (Fig. 2). In both the La Loba (southwestern) domain and the Maravillas (northeastern) domain, rates of dike injection appear to have been sufficient to equalize, or nearly equalize, the magnitudes of principal horizontal stresses. Thus, vent alignments are less common in these domains, and fault slip is less dramatic or absent. In contrast, vent density is generally lower in the El Venado (central) domain (Fig. 9), fault slip is more pronounced, and vent alignments are more obvious. In this area, crustal stresses do not appear to have been completely accommodated by dike-related strain. Thus, synextensional volcanism in the Camargo volcanic field appears to nicely demonstrate the complementary roles of dike injection and faulting in response to regional stress in the southern Basin and Range.

Regional Versus Local Extension, and the Possibility of Active Faulting in Southeast Chihuahua

Our data set on late Cenozoic normal faulting is limited to the Camargo volcanic field and its immediate surroundings. Previous geologic studies of eastern Chihuahua and adjacent Coahuila have indicated that the region belongs either to the Rio Grande rift (Gries, 1979; Seager and Morgan, 1979; Smith and Jones, 1979) or to the Basin and Range province (e.g., papers on Chihuahua in Goodell and Waters, 1981; Henry and Aranda-Gómez, 1992, 2000). However, there are no detailed investigations on the general characteristics and evolution of Cenozoic extension in the region. Extension may have begun before 45 Ma in Chihuahua (e.g., Mauger, 1981; Capps, 1981), was definitely active in the Oligocene–Miocene (Bartolino, 1992) and Pliocene (this paper), and may continue to the present (e.g., Doser and Rodríguez, 1992). By comparison with other areas in northern and central México where more detailed information is available, we assume that extension in Chihuahua-Coahuila occurred in several distinct pulses separated by quasi-quiescent periods and that several pulses of deformation likely affected a given area. Thus, we infer that basin-and-range structures in the Camargo volcanic field were developed in several pulses of activity that cumulatively produced the present-day physiography.

The total vertical fault displacements in the Camargo volcanic field, inferred from the height of the degraded scarps in the central graben and the subtle tilting marked by the playa lakes, indicate low-magnitude Pliocene–Quaternary extension. The lower values of the calculated vertical slip rates (0.03 mm/yr) appear to be consistent with this scenario, because continuous extension since the early Pliocene at this rate would produce vertical displacements of the same order of magnitude as those observed in the central graben (~100 m). On the other hand, the higher slip-rate estimates (0.67–1.67 mm/yr) operating for 3–4 m.y. would have caused unrealistically high vertical displacements on these faults. Thus, we infer that the long-term vertical slip rates in the area must be near the low end of the values obtained. These data are consistent with what little is known about slip rates in the southern Basin and Range province (e.g., Collins et al., 1996). Clear evidence of a close relationship between faulting and volcanic activity, together with the well-documented northeast shift of volcanism in the Camargo volcanic field, suggests that both volcanism and faulting may have occurred in relatively short time spans of rapid and ephemeral activity. Therefore, the high slip rates obtained for some of the Camargo volcanic field faults with very tight time brackets may reflect short intervals with high rates of local down dropping, but do not indicate long-term deformation.

A belt of active faulting has been reported along the Rio Grande, from the region west of El Paso (Nakata et al., 1982) to the Big Bend area (Muehlberger et al., 1978; Henry et al., 1985; Collins et al., 1996). Seismicity in Chihuahua and surrounding regions and the occurrence of at least three large earthquakes of M $>$ 6.3 (Doser and Rodríguez, 1992) indicate that extension is occurring in the region. Therefore, we interpret (1) the youthful geomorphologic features in Sierra San Francisco of the southern El Venado domain, and (2) faults that displace alluvial deposits and late Pleistocene volcanic rocks in the northern Maravillas domain as consistent with the interpretation that extension continues at a low rate in the region.

SUMMARY AND CONCLUSIONS

The Camargo volcanic field formed in the Pliocene–Pleistocene (4.73–0.09 Ma) through hundreds of eruptions of mafic alkalic magmas, some of which carried xenoliths of upper-mantle peridotite and deep-crustal granulite. Compared with other volcanic fields of similar age and composition in the Mexican Basin and Range province, the Camargo volcanic field is unusually large and voluminous, covering ~3000 km^2 with a volume of ~120 km^3. The long-term magmatic eruption rate is estimated at 0.026 km^3/k.y., typical of other mafic alkalic volcanic fields in the Basin and Range province.

The Camargo volcanic field developed where the regional San Marcos fault coincides with an antithetic transfer zone between the opposing San Francisco and Sierra Agua de Mayo fault systems. Volcanism and normal faulting at the Camargo volcanic field were at least in part contemporaneous, and normal faults commonly acted as magmatic conduits in the central graben. Eruptive activity migrated northeastward at ~15 mm/yr. A similar northeast shift may also have occurred in the locus or cessation of Camargo volcanic field faulting.

Minimum vertical slip rates were calculated for four faults in the central graben and range between 0.03 and 1.67 mm/yr. The average slip rate decreases as the age difference between the bracketing samples increases. The larger estimates may approximate slip rates during main faulting intervals, whereas the smaller values better reflect longer-term rates that include long intervals without fault movements. It is likely that the calculated slip rates underestimate the vertical component of the regional extension rate because volcanic activity tends to suppress normal faulting (Parsons and Thompson, 1991) and the transfer zones or bends in a segmented normal fault coincide with displacement minima in the system (Peacock and Sanderson, 1997).

Two different feldspar megacrysts yielded $^{40}Ar/^{39}Ar$ ages identical to groundmass fractions from the same eruptions, demonstrating that such megacrysts can be used to determine reliable eruption ages for their host magmas.

ACKNOWLEDGMENTS

Initial reconnaissance work and compilation of a photogeologic map of the Camargo volcanic field was performed by María Cristina Noyola-Medrano and Marco Antonio Rojas-Beltrán. Gerardo Aguirre, John Stamatakos, Marco Antonio, and Paul Kimberly assisted in the field work. Gustavo Tolson read and commented on an earlier draft of the paper. Ignacio Navarro helped to prepare Figure 9. We gratefully thank them for their assistance. We also thank Luca Ferrari, Max Suter, John Geissman, and John Bartley for the critical comments on the first version of this manuscript, and Gerardo Aguirre-Diaz, Hugo Delgado-Granados, and Lang Farmer for insightful reviews of the revised version. Financial support for this investigation was provided by Consejo Nacional de Ciencia y Tecnología (México) grant 3657PT (to Aranda), the Smithsonian Institution's Scholarly Studies Program (to Luhr), and the U.S. Nuclear Regulatory Commission (NRC) under contract NRC-02-97-009 to the Center for Nuclear Waste Regulatory Analyses (to Connor). This work does not necessarily reflect the views or regulatory position of the NRC.

REFERENCES CITED

Aguirre-Díaz, G.J., and McDowell, F.W., 1991, The volcanic section at Nazas, Durango, México, and the possibility of widespread Eocene volcanism within the Sierra Madre Occidental: Journal of Geophysical Research, v. 96, p. 13,373–13,388.

Almeida-Vega, M., Espinosa-Cardeña, J.M., and Ledesma-Vázquez, J., 2000, Structure of the San Quintín coastal valley, B.C., from aeromagnetic data analysis, *in* Memorias, V Reunión internacional sobre la geología de la península da Baja California: Loreto, Baja California Sur, México, Sociedad Geológica Peninsular, p. 64.

Aranda-Gómez, J.J., Henry, C.D., Luhr, J.F., and McDowell, F.W., 1997, Cenozoic volcanism and tectonics in northwest Mexico: A transect across the Sierra Madre Occidental volcanic field and observations on extension related magmatism in the southern Basin and Range and Gulf of California tectonic provinces, *in* Aguirre-Díaz, G.J., Aranda-Gómez, J.J., Carrasco-Nuñez, G., and Ferrari, L., eds., Magmatism and tectonics in the central and northwestern Mexico: A selection of the 1997 IAVCEI General Assembly excursions: México, D.F., Universidad Nacional Autónoma de México, Instituto de Geología, Excursión 11, p. 41–84.

Aspen, J., Upton, B.G.J., and Dickin, A.P., 1990, Anorthoclase, sanidine and associated megacrysts in Scottish alkali basalts: High-pressure syenitic debris from upper mantle sources?: European Journal of Mineralogy, v. 2, p. 503–517.

Axen, G.J., Taylor, W.J., and Bartley, J.M., 1993, Space-time patterns and tectonic controls of Tertiary extension and magmatism in the Great Basin of the western United States: Geological Society of America Bulletin, v. 105, p. 56–76.

Bailey, D.K., 1974, Continental rifting and alkaline magmatism, *in* Sorensen, H., ed., The alkaline rocks: New York, John Wiley and Sons, p. 148–159.

Bartolino, J.R., 1992, Modified Basin and Range topography in the Bolsón de Mapimi, Durango and Chihuahua, México: The Texas Journal of Science, v. 44, no. 3, p. 295–300.

Binns, R.A., 1969, High-pressure megacrysts in basanitic lavas near Armidale, New South Wales: American Journal of Science, v. 267-A, p. 33–49.

Cameron, K., and Jones, N., 1993, A reconnaissance Nd-Sr isotopic study of pre-Cenozoic igneous and metaigneous rocks of the Coahuila terrane, northeastern Mexico, *in* Ortega-Gutiérrez, F., Coney, P.J., Centeno-García, E., and Gómez-Caballero, A., eds., First Circum-Pacific and Circum-Atlantic Terrane Conference, Proceedings: Guanajuato, México, Universidad Nacional Autónoma de México, Instituto de Geología, p. 24–27.

Cameron, K.L., Clark, L.F., and Cameron, M., 1983, A preliminary report on the nature of the lower crust and upper mantle beneath southeastern Chihuahua: El Paso Geological Society Guidebook, p. 102–107.

Cameron, K.L., Robinson, J.V., Niemeyer, S., Nimz, G.J., Kuentz, D.C., Harmon, R.S., Bohlen, S.R., and Collerson, K.D., 1992, Contrasting styles of pre-Cenozoic and mid-Tertiary crustal evolution in northern México: Evidence from deep crustal xenoliths from La Olivina: Journal of Geophysical Research, v. 97, p. 17,353–17,376.

Capps, R.C., 1981, Geology of the Rancho El Papalote area, Chihuahua, Mexico, *in* Goodell, P.C., and Waters, A.C., eds., Uranium in volcanic and volcaniclastic rocks: Tulsa, Oklahoma, American Association of Petroleum Geologists Studies in Geology 13, p. 243–264.

Comision de Estudios del Territorio Nacional (Cetenal), 1974, El Milagro G13B22: México, D.F., Secretaría de la Presidencia, Comisión de Estudios del Territorio Nacional, Topographic quadrangle, scale 1:50,000, 1 sheet.

Collins, E.W., Raney, J.A., Machette, M., Haller, K.M., and Dart, R.L., 1996, Map and data for Quaternary faults in West Texas and adjacent parts of Mexico: U.S. Geological Survey Open-File Report 96–002, 7 p.

Condit, C.D., and Connor, C.B., 1996, Recurrence rates of volcanism in basaltic volcanic fields: An example from the Springerville volcanic field, Arizona: Geological Society of America Bulletin, v. 108, p. 1225–1241.

Condit, C.D., Crumpler, L.S., and Aubele, J.C., 1989a, Fourth-day field trip: Springerville volcanic field, *in* Chapin, C.E., and Zedik, J., eds., Field excursions to volcanic terranes in the Western United States, Volume I: Southern Rocky Mountain region: New Mexico Bureau of Mines and Mineral Resources Memoir 4, p. 33–41.

Condit, C.D., Crumpler, L.S., Aubele, J.C., and Elston, W.E., 1989b, Patterns of volcanism along the southern margin of the Colorado Plateau: The Springerville field: Journal of Geophysical Research, v. 94, p. 7975–7986.

Coney, P.J., and Campa, M.F., 1987, Lithotectonic terrane map of México (west of the 91st meridian): U.S. Geological Survey Miscellaneous Field Studies Map MF-1874-D, scale 1:2,500,000.

Connor, C.B., 1990, Cinder cone clustering in the TransMexican volcanic belt: Implications for structural and petrologic models: Journal of Geophysical Research, v. 95, p. 19395–19405.

Connor, C.B., and Conway, F.M., 2000, Basaltic volcanic fields, *in* Sigurdsson, H., ed., Volcano encyclopedia: New York, Academic Press, p. 331–343.

Conway, F.M., Ferrill, D.A., Hall, C.M., Morris, A.P., Stamatakos, J.A., Connor, C.B., Halliday, A.N., and Condit, C.D., 1997, Timing of basaltic volcanism along the Mesa Butte fault in the San Francisco volcanic field, Arizona from $^{40}Ar/^{39}Ar$ dates: Implications for the longevity of cinder cone alignments: Journal of Geophysical Research, v. 102, p. 815–824.

Crisp, J.A., 1984, Rates of magma emplacement and volcanic output: Journal of Volcanology and Geothermal Research, v. 20, p. 177–211.

Doser, D.I., and Rodríguez, J., 1992, The seismicity of Chihuahua, México and surrounding regions: Guidebook for the 1992 Field Conference, El Paso Geological Society, p. 99–105.

Dungan, M.A., Lindstrom, M.M., McMillan, N.J., Moorbath, S., Hoefs, J., and Haskin, L.A., 1986, Open system magmatic evolution of the Taos Plateau volcanic field, northern New Mexico: 1. The petrology and geochemistry of the Servilleta basalt: Journal of Geophysical Research, v. 91, p. 5999–6028.

Foland, K.A., 1974, Ar 40 diffusion in homogeneous orthoclase and an interpretation of Ar diffusion in K-feldspars: Geochimica et Cosmochimica Acta, v. 38, p. 151–166.

Gans, P.B., Mahood, G.A., and Schermer, E., 1989, Synextensional magmatism in the Basin and Range province: A case study from the eastern Great Basin: Geological Society of America Special Paper 233, p. 1–53.

Glazner, A.F., and Bartley, J.M., 1994, Eruption of alkali basalts during crustal shortening in southern California: Tectonics, v. 13, p. 493–498.

Goodell, P.C., and Waters, A.C., 1981, Uranium in volcanic and volcaniclastic rocks: American Association of Petroleum Geologists Studies in Geology 3, 331 p.

Grajales-Nishimura, J.M., Terrell, D.J., and Damon, P.E., 1992, Evidencias de la prolongación del arco magmático cordillerano del Triásico–Jurásico en Chihuahua, Durango y Coahuila: Boletín de la Asociación

Mexicana de Geológos Petroleros, v. XLII, no. 2, p. 1–18.

Gries, J.C., 1979, Problems of delineation of the Rio Grande rift into the Chihuahua tectonic belt of northeastern Mexico, *in* Riecker, R.E., ed., The Rio Grande rift—Tectonics and magmatism: Washington, D.C., American Geophysical Union, p. 107–113.

Harrison, T.M., 1990, Some observations on the interpretation of feldspar ^{40}Ar-^{39}Ar results: Chemical Geology, v. 80, p. 219–229.

Hasenaka, T., and Carmichael, I.S.E., 1985, The cinder cones of Michoacán-Guanajuato, central México: Their age, volume and distribution, and magma discharge rate: Journal of Volcanology and Geothermal Research, v. 25, p. 105–124.

Henry, C.D., and Aranda-Gómez, J.J., 1992, The real southern Basin and Range: Mid to late Cenozoic extension in Mexico: Geology, v. 20, p. 701–704.

Henry, C.D., and Aranda-Gómez, J.J., 2000, Plate interactions control middle–late Miocene, proto-Gulf and Basin and Range extension in the southern Basin and Range: Tectonophysics, v. 318, p. 1–26.

Henry, C.D., Gluck, J.K., and Bockoven, N.T., 1985, Tectonic map of the Basin and Range province of Texas and adjacent Mexico: Austin, University of Texas, Bureau of Economic Geology, Miscellaneous Map 36, scale 1:500,000.

Irving, A.J., 1974, Megacrysts from the Newer Basalts and other basaltic rocks from southeastern Australia: Geological Society of America Bulletin, v. 85, p. 1503–1514.

Keller, E.A., 1986, Investigation of active tectonics: Use of surficial earth processes, *in* Active tectonics: Washington, D.C., National Academy Press, p. 136–147.

Luhr, J.F., Aranda-Gómez, J.J., and Pier, J.G., 1989, Spinel-lherzolite-bearing, Quaternary volcanic centers in San Luis Potosí, México: I. Geology, mineralogy, and petrology: Journal of Geophysical Research, v. 94, p. 7916–7940.

Luhr, J.F., Pier, J.G., Aranda-Gómez, J.J., and Podosek, F., 1995a, Crustal contamination in early Basin-and-Range hawaiites of the Los Encinos volcanic field, central México: Contributions to Mineralogy and Petrology, v. 118, p. 321–339.

Luhr, J.F., Aranda-Gómez, J.J., and Housh, T.B., 1995b, The San Quintín volcanic field, Baja California Norte, México: Geology, petrology, and geochemistry: Journal of Geophysical Research, v. 100, p. 10353–10380.

Luhr, J.F., Henry, C.D., Housh, T.B., Aranda-Gómez, J.J., and McIntosh, W.C., 2001, Early extension and associated mafic alkalic volcanism from the southern Basin and Range province: Geology and petrology of the Rodeo and Nazas volcanic fields, Durango (Mexico): Geological Society of America Bulletin, v. 113, p. 760–773.

Mauger, R.L., 1981, Geology and petrology of the central part of the Calera–Del Nido block, Chihuahua, Mexico, *in* Goodell, P.C., and Waters, A.C., eds., Uranium in volcanic and volcaniclastic rocks: American Association of Petroleum Geologists Studies in Geology 13, p. 205–242.

McCalpin, J.P., 1995, Frequency distribution of geologically determined slip rates for normal faults in the western United States: Bulletin of the Seismological Society of America, v. 85, p. 1867–1872.

McDowell, F.W., and Keizer, R.P., 1977, Timing of mid-Tertiary volcanism in the Sierra Madre Occidental between Durango City and Mazatlan, México: Geological Society of America Bulletin, v. 88, p. 1479–1486.

McKee, J.W., and Jones, N.W., 1979, A large Mesozoic fault in Coahuila, Mexico: Geological Society of America Abstracts with Programs, v. 11, p. 476.

McKee, J.W., Jones, N.W., and Long, L.E., 1984, History of recurrent activity along a major fault in northeastern México: Geology, v. 12, p. 103–107.

McKee, J.W., Jones, N.W., and Long, L.E., 1990, Stratigraphy and provenance of strata along the San Marcos fault, central Coahuila, México: Geological Society of America Bulletin, v. 102, p. 593–614.

Muehlberger, W.R., Belcher, R.C., and Goetz, L.K., 1978, Quaternary faulting in Trans-Pecos Texas: Geology, v. 6, p. 337–340.

Nakata, J.K., Wentworth, C.M., and Machette, M.N., 1982, Quaternary fault map of the Basin and Range and Rio Grande rift provinces, western United States: U.S. Geological Survey Open-File Report 82–579, scale 1: 2,500,000.

Nielson, R.L., and Dungan, M.A., 1985, The petrology and geochemistry of the Ocate volcanic field, north-central New Mexico: Geological Society of America Bulletin, v. 96, p. 296–312.

Nieto-Samaniego, A.F., Ferrari, L., Alaniz-Alvarez, S.A., Labarthe-Hernández, G., and Rosas-Elguera, J.G., 1999, Variation of Cenozoic extension and volcanism across the southern Sierra Madre Occidental volcanic province, México: Geological Society of America Bulletin, v. 111, p. 347–363.

Nimz, G.J., Cameron, K.L., Cameron, M., and Morris, S.L., 1986, The petrology of the lower crust and upper mantle beneath southeastern Chihuahua, México: A progress report: Geofísica Internacional, v. 25, no. 1, p. 85–116.

Nimz, G.J., Cameron, K.L., and Niemeyer, S., 1993, The La Olivina pyroxenite suite and the isotopic compositions of mantle basalts parental to mid-Cenozoic arc volcanism of northern México: Journal of Geophysical Research, v. 98, p. 6489–6509.

Nimz, G.J., Cameron, K.L., and Niemeyer, S., 1995, Formation of mantle lithosphere beneath northern México: Chemical and Sr-Nd-Pb isotopic systematics of peridotite xenoliths from La Olivina: Journal of Geophysical Research, v. 100, p. 4181–4196.

Noyola-Medrano, M.C., 1995, Estudio comparativo de la geología y morfología de algunos conos cineríticos en los Campos Volcánicos de Camargo, Chih. y San Quintín, B.C., [B.S. thesis]: San Luis Potosí, México, Universidad Autónoma de San Luis Potosí, 91 p.

Padilla y Sánchez, R.J., 1986, Post-Paleozoic tectonics of northeast Mexico and its role in the evolution of the Gulf of Mexico: Geofísica Internacional, v. 25, no. 1, p. 157–206.

Parsons, T., and Thompson, G.A., 1991, The role of magma overpressure in suppressing earthquakes and topography: Worldwide examples: Science, v. 253, p. 1399–1402.

Paterson, S.R., and Schmidt, K.L., 1999, Is there a close spatial relationship between faults and plutons?: Journal of Structural Geology, v. 21, p. 1131–1142.

Peacock, D.C.P., and Sanderson, D.J., 1997, Geometry and development of normal faults, *in* Sengupta, S., ed., Evolution of geological structures in micro- to macroscales: London, Chapman and Hall, p. 27–46.

Rudnick, R.L., and Cameron, K.L., 1991, Age diversity of the deep crust in northern México: Geology, v. 19, p. 1197–1200.

Schmidt, K.L., and Paterson, S.R., 2000, Analyses fail to find coupling between deformation and magmatism: Eos (Transactions, American Geophysical Union), v. 81, p. 197–203.

Seager, W.R., and Morgan, P., 1979, Rio Grande rift in southern New Mexico, west Texas, and northern Chihuahua, *in* Riecker, R.E., ed., The Rio Grande rift—Tectonics and magmatism: Washington, D.C., American Geophysical Union, p. 87–106.

Sedlock, R.L., Ortega-Gutiérrez, F., and Speed, R.C., 1993, Tectonostratigraphic terranes and tectonic evolution of México: Geological Society of America Special Paper, v. 278, 153 p.

Sharp, W.D., Turrin, B.D., Renne, P.R., and Lanphere, M.A., 1996, The $^{40}Ar/^{39}Ar$ and K/Ar dating of lavas from the Hilo 1-km core hole, Hawaii Scientific Drilling Project: Journal of Geophysical Research, v. 101, p. 11,607–11,616.

Smith, J.A., 1989, Extension-related magmatism of the Durango volcanic field, Durango, México [M.A. thesis]: St. Louis, Missouri, Washington University, 102 p.

Smith, R.D., 1993, The Agua de Mayo mid-Cenozoic volcanic group and related xenoliths from La Olivina southeast Chihuahua, México [M.S. thesis]: Santa Cruz, University of California, 112 p.

Smith, D.L., and Jones, R.L., 1979, Thermal anomaly in northern Mexico: An extension of the Rio Grande rift?, *in* Riecker, R.E., ed., The Rio Grande rift—Tectonics and magmatism: Washington, D.C., American Geophysical Union, p. 269–278.

Smith, R.D., Cameron, K.L., McDowell, F.W., Niemeyer, S., and Sampson, D.E., 1996, Generation of voluminous silicic magmas and formation of mid-Cenozoic crust beneath north-central México: Evidence from ignimbrites, associated lavas, deep crustal granulites, and mantle pyroxenites: Contributions to Mineralogy and Petrology, v. 123, p. 375–389.

Sociedad Geológica Mexicana A.C., D.C., 1985, Plano geológico minero Chihuahua, México: Consejo de Recursos Minerales, scale 1:500,000, 1 sheet.

Swanson, E.R., Keizer, R.P., Lyons, J.I., and Clabaugh, S.E., 1978, Tertiary volcanism and caldera development near Durango City, Sierra Madre Occidental, México: Geological Society of America Bulletin, v. 89, p. 1000–1012.

Tanaka, K.L., Shoemaker, E.M., Ulrich, G.E., and Wolfe, E.W., 1986, Migration of volcanism in the San Francisco volcanic field, Arizona: Geological Society of America Bulletin, v. 97, p. 129–141.

Tarango-Ontiveros, G., 1993, Bosquejo geológico de la porción surcentral del Estado de Chihuahua, *in* III Excursión geológica al Mesozoico de Chihuahua (Chihuahua-Parral-Jiménez-Chihuahua): Chihuahua, Sociedad Geológica Mexicana, Delegación Chihuahua, p. 2–10.

Manuscript Received by the Society 28 June 2001
Revised Manuscript Received 1 May 2002
Manuscript Accepted 9 July 2002

Printed in the USA